

# 1 A Sustainable Approach for the Synthesis of Catalytically Active 2 Peroxidase-Mimic ZnS Catalysts

3 Camilla M. Cova,<sup>†</sup> Alessio Zuliani,<sup>†</sup> Mario J. Muñoz-Batista,<sup>†</sup> and Rafael Luque<sup>\*,†,‡,§</sup>

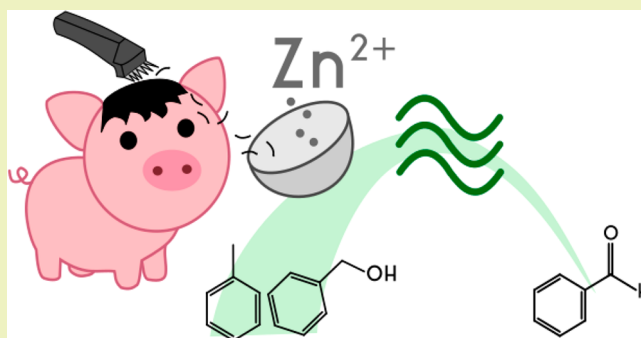
4 <sup>†</sup>Departamento de Química Orgánica, Universidad de Córdoba, Edificio Marie-Curie (C-3), Ctra Nnal IV-A, Km 396, E-14014  
5 Córdoba, Spain

6 <sup>‡</sup>Peoples Friendship University of Russia (RUDN University), 6 Miklukho-Maklaya str., 117198, Moscow, Russia

7 **S** Supporting Information

8 **ABSTRACT:** Zinc sulfides are emerging as promising  
9 catalysts in different fields such as photochemistry or organic  
10 synthesis. Nevertheless, the synthesis of ZnS compounds  
11 normally requires the utilization of toxic sulfur precursors, e.g.,  
12 thiourea which is a contaminant and carcinogenic agent. As a  
13 result, new green and sustainable synthetic methodologies are  
14 needed. Herein, an innovative, simple, and cheap approach for  
15 the synthesis of ZnS carbon composites is reported. Zinc  
16 acetate dihydrate was employed as metal precursor while  
17 wasted pig bristles were employed as carbon and sulfur source.  
18 The phase and the morphology of the compounds were  
19 analyzed by XRD, XPS, SEM, and EDX and the surface area  
20 was determined by nitrogen physisorption. ZnS carbon  
21 materials showed remarkable peroxidase-like catalytic activity for two different model reactions: the liquid-phase selective  
22 oxidation of benzyl alcohol and toluene to benzaldehyde (conversions up to 63% and 29% and selectivities up to 86% and 87%,  
23 respectively) using hydrogen peroxide as oxidant under microwave irradiation.

24 **KEYWORDS:** Zinc sulfide, Pig bristles, Microwave chemistry, Selective oxidations



## 25 ■ INTRODUCTION

26 Zinc sulfide has been studied as an important compound due  
27 to its unique physical and photochemical properties.<sup>1–3</sup> It has  
28 demonstrated an extraordinary versatility and potentiality for  
29 different applications including light-emitting diodes (LEDs),  
30 electroluminescence, infrared windows, sensors, lasers, and  
31 biodevices.<sup>4–6</sup> Additionally, ZnS possesses many interesting  
32 characteristics such as excellent transport properties, an  
33 intrinsically *n*-type semiconductivity, good thermal stability,  
34 high electronic mobility, nontoxicity, water insolubility, and  
35 low-production costs.<sup>4–7</sup>

36 All reported synthetic protocols for ZnS preparation involve  
37 the utilization of highly toxic sulfur sources including extremely  
38 hazardous compounds such as H<sub>2</sub>S, or Na<sub>2</sub>S as well as  
39 thioureas, highly contaminant and carcinogenic agents.<sup>8–10</sup>  
40 New green and low-toxicity sulfur sources are therefore  
41 required for sustainable development. In this context, pig  
42 bristles represent a cheap and largely available source of sulfur  
43 (and carbon). Pig bristles are considered as a waste toxic-free  
44 feedstock, easily collectable and accessible at industrial scale. In  
45 fact, ca. ~225k tons of wasted pig bristles are yearly produced  
46 only in European slaughterhouses.<sup>11</sup> However, only a few  
47 works to date are available on the reutilization/use of pig  
48 bristles as food fodder supplements, while their valorization as  
49 chemical source is extremely limited.<sup>11–13</sup>

Herein, a simple and innovative synthesis of ZnS carbon  
50 composites derived from wasted pig bristles is reported. The  
51 synthetic procedure involved a facile heating step in a diluted  
52 aqueous solution of potassium hydroxide. Wasted pig bristles  
53 were employed as sulfur and carbon source while zinc acetate  
54 dihydrate was used as metal source. The material was  
55 characterized by XPS, XRD, N<sub>2</sub> physisorption, SEM, and  
56 EDX, demonstrating the successful formation of zinc sulfides  
57 carbon compounds.<sup>58</sup>

In order to validate the practical application of the new  
59 material, ZnS carbon composites were tested as catalysts in two  
60 different model reactions: the selective oxidation of benzyl  
61 alcohol and toluene to benzaldehyde. Among all known  
62 oxidative transformations, the selective oxidations of alcohols  
63 to the corresponding carbonyl compounds have gained  
64 attention due to their broad range of industrial applica-  
65 tions.<sup>14,15</sup> Specifically, the conversion of benzyl alcohol to  
66 benzaldehyde has attracted significant interest since benzalde-  
67 hyde is a widely used chemical in food, pharmaceutical, and  
68 perfumery industries as well as building block in other  
69 chemical industries.<sup>16–22</sup> For example, benzaldehyde is  
70 commonly used as a flavor and fragrance agent tasting of 71

**Received:** September 27, 2018

**Revised:** November 5, 2018

**Published:** December 7, 2018

72 almond, peach, marzipan, and pistachio. In addition,  
 73 benzaldehyde can be also synthesized via toluene oxidation.<sup>23</sup>  
 74 Considering that toluene is classified as a highly pollutant  
 75 chemical, its oxidation to beneficial chemicals products, i.e.,  
 76 benzyl alcohol, benzaldehyde, benzoic acid, and benzoate, is  
 77 extremely attractive.<sup>24,25</sup> For example, benzoic acid is  
 78 industrially obtained from toluene using (thermally driven)  
 79 Co-based catalyzed reactions.<sup>26</sup>  
 80 ZnS carbon compounds were particularly tested in fast  
 81 microwave-assisted reactions, using only hydrogen peroxide as  
 82 oxidant. Less aggressive oxidants such as hydrogen peroxide  
 83 ( $\text{H}_2\text{O}_2$ ) and molecular oxygen ( $\text{O}_2$ ) are nowadays employed  
 84 aiming to scale up oxidation processes,<sup>14</sup> whereas, in the past,  
 85 the scale up of the oxidation reactions has been very limited  
 86 due to the use of heavy metals (e.g., chromium, manganese,  
 87 and permanganate derivatives).<sup>27–30</sup> In addition, the utilization  
 88 of hydrogen peroxide allows the minimization of chemical  
 89 waste in these catalytic processes, as water is the only reaction  
 90 side product.

## 91 ■ MATERIALS AND METHODS

92 **Materials.** Zinc acetate dihydrate ( $\text{Zn}(\text{CH}_3\text{COOH})_2 \cdot 2\text{H}_2\text{O}$ ),  
 93 potassium hydroxide (KOH), acetone ( $\text{CH}_3\text{COCH}_3$ ), ethanol  
 94 ( $\text{CH}_3\text{CH}_2\text{OH}$ , 99.8%), acetonitrile ( $\text{CH}_3\text{CN}$ , 99.8%), benzyl alcohol  
 95 ( $\text{C}_6\text{H}_5\text{CH}_2\text{OH}$ , 99.8%), toluene ( $\text{C}_7\text{H}_8$ , 99.8%), and hydrogen  
 96 peroxide ( $\text{H}_2\text{O}_2$ , 30% v/v) were purchased from Sigma-Aldrich Inc.,  
 97 St. Louis, MO, USA. All reagents were used without any further  
 98 purification.

99 **Synthesis of ZnS Carbon Catalysts.** A sequence of three ZnS  
 100 carbon structures characterized by different synthesis times were  
 101 prepared. In a typical procedure, the correct amount of zinc acetate  
 102 dihydrate (850 mg, 3.8 mmol) was dissolved in 200 mL of 1.0 M  
 103 KOH solution in a 250 mL round flask equipped with a stirring bar  
 104 and a reflux condenser. Sequentially, 1.5 g of pig bristles (cut in pieces  
 105 of  $\sim 5$  mm) was added. The mixture was kept at room temperature  
 106 under vigorous magnetic stirring (800 rpm) for 10 min before starting  
 107 the reaction. The mixture was then heated at reflux in an oil bath.  
 108 After completing the reaction, the solution was naturally cooled down  
 109 to r.t. and the light-brown precipitate was filtrated and washed several  
 110 times with acetone and ethanol. Finally, the material was oven-dried  
 111 at 100 °C for 24 h. Three different samples were produced by setting  
 112 the heating time for 1 h, 3 h, and 5 h. The samples were denoted ZnS-  
 113 1h, ZnS-3h, and ZnS-5h, respectively.

114 **Material Characterization.** ZnS carbon composites were  
 115 characterized by scanning electron microscopy (SEM), energy  
 116 dispersive X-ray analysis (EDX), powder X-ray diffraction (XRD),  
 117  $\text{N}_2$  physisorption, and X-ray photoelectronic spectroscopy (XPS).

118 Scanning electron microscopy images were recorded with a JEOL  
 119 JSM-6300 scanning microscope (JEOL Ltd., Peabody, MA, USA)  
 120 equipped with energy-dispersive X-ray spectroscopy (EDX) of 15 kV  
 121 at the Research Support Service Center (SCAI) from University of  
 122 Cordoba.

123 Powder X-ray diffraction (XRD) patterns were recorded using a  
 124 Bruker D8 DISCOVER A25 diffractometer (PanAnalytic/Philips,  
 125 Lelyweg, Almelo, The Netherlands) using  $\text{Cu K}\alpha$  ( $\lambda = 1.5418 \text{ \AA}$ )  
 126 radiation. Wide angle scanning patterns were collected over a  $2\theta$   
 127 range from 10° to 80° with a step size of 0.018° and counting time of  
 128 5 s per step.

129 Textural properties of the samples were determined by  $\text{N}_2$   
 130 physisorption using a Micromeritics ASAP 2020 automated system  
 131 (Micromeritics Instrument Corporation, Norcross, GA, USA) with  
 132 the Brunauer–Emmet–Teller (BET) and the Barrett–Joyner–  
 133 Halenda (BJH) methods. Prior to analysis, the samples were  
 134 outgassed for 24 h at 100 °C under vacuum ( $P_0 = 10^{-2} \text{ Pa}$ ) and  
 135 subsequently analyzed.

136 XPS studies were performed at the Central Service of Research  
 137 Support (SCAI) of the University of Cordoba, using an ultrahigh

vacuum (UHV) multipurpose surface analysis system Specs. The  
 138 experiments were carried out at pressures  $< 10^{-10}$  mbar, using a  
 139 conventional X-ray source (XR-50, Specs, Mg-K $\alpha$ ,  $h\nu = 1253.6 \text{ eV}$ ,  
 140  $1 \text{ eV} = 1.603 \times 10^{-19} \text{ J}$ ) in a “stop and go” mode. The samples were  
 141 deposited on a sample holder using a double sided adhesive tape, and  
 142 afterward evacuated overnight under vacuum ( $< 10^{-6}$  mbar). Spectra  
 143 were collected at room temperature (pass energy: 25 and 10 eV, step  
 144 size: 1 and 0.1 eV) with a Phoibos 150-MCD energy detector. The  
 145 deconvolutions of the obtained curves and element quantification  
 146 were carried out using XPS CASA program. 147

**Catalytic Activity.** The oxidation tests were performed following  
 148 a procedure optimized in a previous work.<sup>31</sup> Briefly, 25 mg of catalyst,  
 149 0.1 mL of benzyl alcohol (0.95 mmol) or 0.1 mL of toluene (0.94  
 150 mmol), 0.25 mL of hydrogen peroxide (30% v/v), and 2 mL of  
 151 acetonitrile as solvent. Blank tests were run in the absence of the  
 152 catalysts. Both microwave-assisted oxidations were carried out in a  
 153 CEM-Discover microwave reactor, equipped with a PC-controlled  
 154 interface. The mixtures were irradiated for 45 min, withdrawing  
 155 aliquots for GC-FID analysis every 15 min. The experiments were  
 156 performed in closed vessels. The “discover” method was used under  
 157 pressure, allowing the control of the irradiation power, the  
 158 temperature, and the pressure. The reactions were stirred and heated  
 159 with microwave irradiation, fixing the temperature at 120 °C by an  
 160 infrared probe. The autogenous pressure ranged from 3.5 to 8 bar. 161

**Product Analysis.** The filtrates collected from the reaction  
 162 mixtures were analyzed by GC, using an Agilent 19091J-413 GC  
 163 model equipped with a Supelco 2-8047-U (30 m  $\times$  0.32 mm  $\times$  0.25  
 164  $\mu\text{m}$  i.d.) capillary column and an FID detector. The temperature of  
 165 the column was ramped at 25 °C  $\text{min}^{-1}$  to 25 °C (1 min hold time),  
 166 then at 25 °C  $\text{min}^{-1}$  to 250 °C (5 min hold time), and finally to 300  
 167 °C at 20 °C  $\text{min}^{-1}$  (10 min hold time). The nitrogen gas flow was set  
 168 at 1.3 mL  $\text{min}^{-1}$ . 169

## 170 ■ RESULTS AND DISCUSSION

**Synthesis of ZnS Carbon Composites.** A simple, fast,  
 171 and cheap methodology is shown for the synthesis of ZnS  
 172 carbon structures using wasted pig bristles as carbon and sulfur  
 173 source. As reported by Gonzalo et al., pig bristles are carbon-  
 174 and sulfur-rich wastes largely produced in most industrialized  
 175 countries, generally burnt as waste or partially reused in brush  
 176 industries or as food fodder supplement.<sup>12,13,32</sup> The sulfur  
 177 contained in pig bristles is mainly derived from keratin, an  
 178 insoluble protein containing disulfide bonds as well as from  
 179 amino acids such as cysteine, methionine, and cysteic acid.<sup>33</sup>  
 180 Due to similarities with human hair, the total amount of sulfur  
 181 contained in pig bristles has been reported to be ca. 5% wt.<sup>34</sup>  
 182 However, contrary to human hair, which production is also  
 183 vast but distributed in the numerous barber shops, pig bristles  
 184 are produced in large quantities in slaughterhouses and can be  
 185 easily collected at industrial scale. 186

As illustrated in Figure 1, the new synthesis involved a  
 187 unique step where a mixture of pig bristles, zinc acetate 188



**Figure 1.** Schematic illustration of the preparation of ZnS.

dihydrate, and a solution 1.0 M of potassium hydroxide was  
 189 heated up under reflux conditions. 190

The synthesis is adapted from a previously reported protocol  
 191 for the preparation of  $\text{Cu}_2\text{S}$ , where the solvent solution, made  
 192 of ethylene glycol and NaOH, has been substituted with a less  
 193 hazardous and easier to manipulate dilute aqueous solution of  
 194 KOH.<sup>11</sup> Ethylene glycol is indeed a suspicious carcinogenic 195



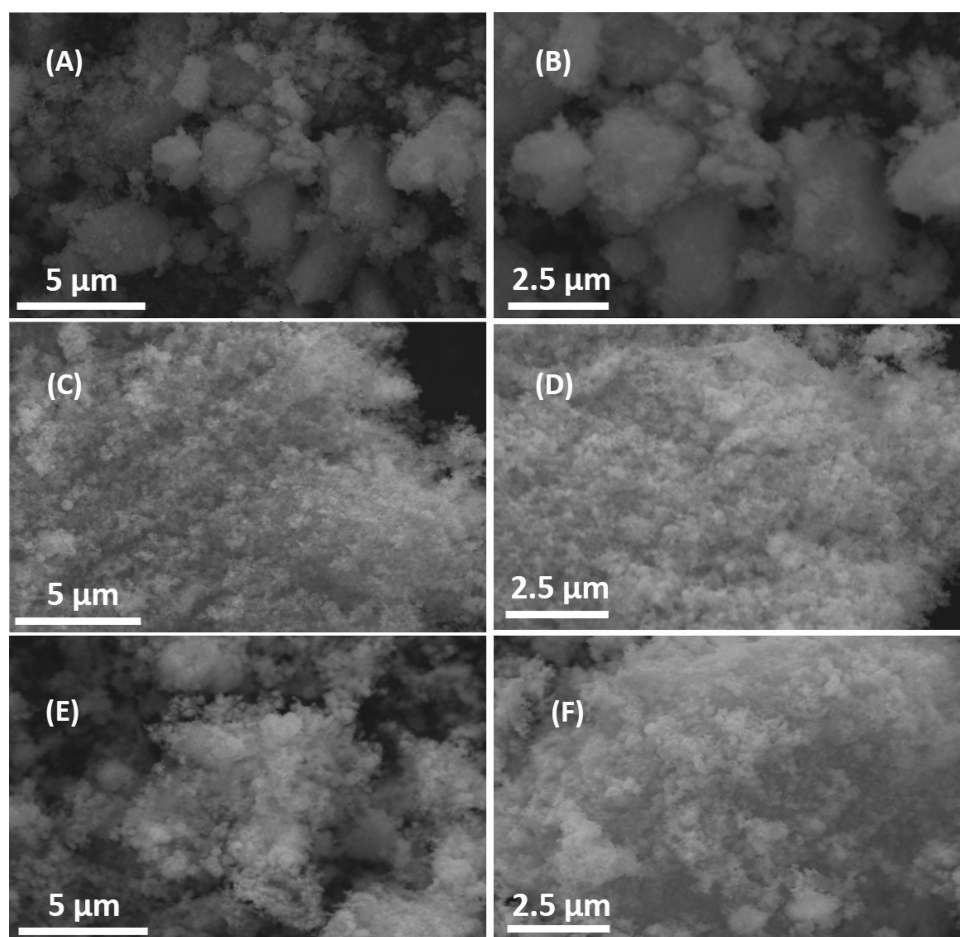


Figure 2. SEM images of the three different ZnS composites. (A, B) ZnS-1h; (C, D) ZnS-3h; (E, F) ZnS-5h.

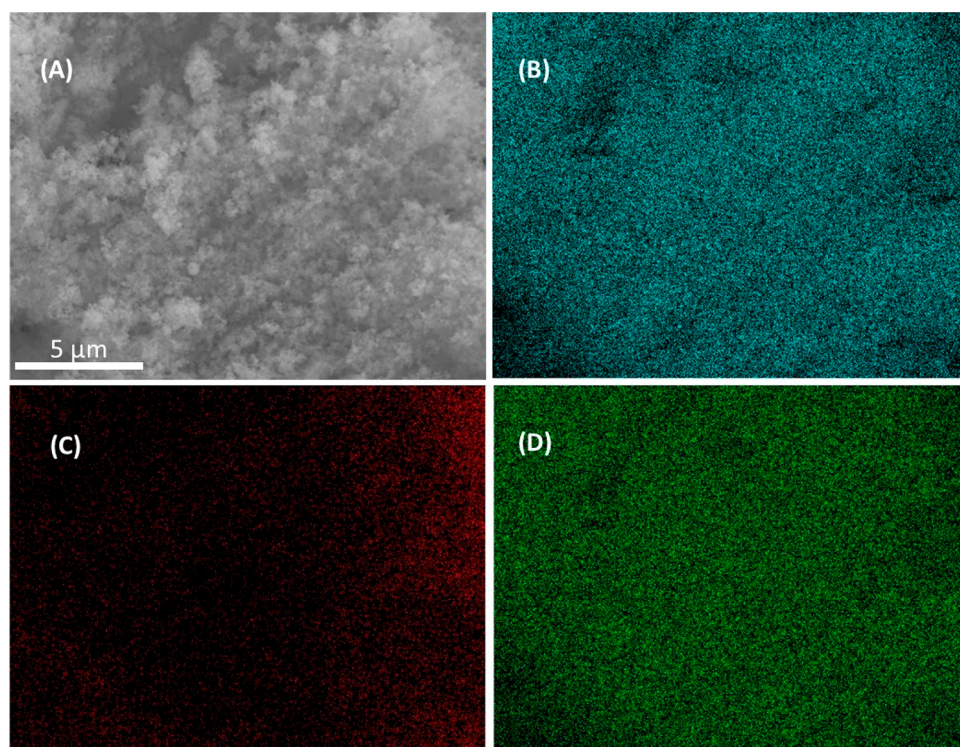


Figure 3. SEM images of ZnS-3h with mapping analysis of (A) ZnS carbon structure, (B) zinc, (C) carbon, and (D) sulfur.

196 agent and can explosively degrade when heated up with  
197 NaOH. The aqueous basic solution of KOH was employed in  
198 order to accelerate and facilitate the decomposition of pig  
199 bristles and the release of sulfur via keratin hydrolysis.<sup>35</sup>  
200 Without the basic solution, the thermal degradation would  
201 require higher temperature and processing time. In fact, keratin  
202 and amino acids present in proteins start to thermally degrade  
203 above 150 °C, and release sulfur up to 300 °C.<sup>36</sup>

204 When the mixture was heated up, the pig bristles started to  
205 decompose and the dissolved Zn<sup>2+</sup> ions bind with sulfur.  
206 During this step, the particles self-aggregate in order to  
207 minimize the surface energy, incorporating the residual carbon,  
208 and forming homogeneous ZnS carbon structures. Three  
209 different samples were prepared, using the same amount of pig  
210 bristles and zinc acetate dihydrate and heating up the reaction  
211 mixture for different times, respectively 1 h, 3 h, and 5 h. The  
212 zinc sulfide carbon materials were denoted as ZnS-1h, ZnS-3h,  
213 and ZnS-5h.

214 **Materials Characterization.** The morphology of ZnS  
215 carbon structures was investigated by SEM and EDX analyses.  
216 Figure 2 shows SEM images for the three ZnS carbon  
217 materials. All samples exhibited a “coral-like” homogeneous  
218 morphology where the carbon derived from the degradation of  
219 pig bristles was aggregated with ZnS. EDX mappings were  
220 reported in order to demonstrate the distribution of catalyti-  
221 cally active sites, as reported in Figure 3 for sample ZnS-3h.<sup>37</sup>  
222 Remarkably, zinc, sulfur, and carbon were found to be well  
223 distributed in the material, confirming the homogeneous  
224 conditions of the synthesis, and the presence of active sites  
225 over all the catalyst surface (please see Figures S1 and S2 for  
226 ZnS-1h and ZnS-5h EDX mapping).

227 EDX-mapping micrographs showed the presence of carbon,  
228 sulfur, and zinc, indicating the high purity of the materials. The  
229 phase purity and crystallinity of synthesized ZnS carbon  
230 composites were subsequently investigated by XRD analysis.  
231 As shown in Figure 4, XRD patterns for all different samples  
232 showed the presence of zinc sulfide. The diffraction peaks at  
233 29.04°, 48.38°, and 57.42° could be indexed to the (1 1 1), (2  
234 2 0), and (3 1 1) planes of cubic zinc sulfide (JCPDS 01-080-  
235 0020).<sup>38</sup> No other impurity peaks detected through XRD also  
236 suggested high purity in the materials. In addition, the width of  
237 the most intense peaks at half height measured almost the

same for the three patterns, indicating similar dimensions of  
the particles in all the samples, according to Scherrer's  
equation.

The samples were thus subjected to an XPS study. Figure 5  
shows plots of high-resolution spectra concerning C 1s, Zn 2p,  
and S 2p regions. A summary of the fitting position values for  
the different elements mentioned as well as the surface atomic  
ratios (C/Zn) is presented in Table 1. In agreement with XRD  
analysis, the presence of a defined ZnS structure was  
successfully observed for all synthesized ZnS materials. In  
particular, both Zn 2p and S 2p core level spectra do not  
display significant modifications with synthesis time (middle  
and right panels of Figure 5). Zn 2p shows two strong peaks at  
ca. 1021.5 and 1044.8 eV, assigned to the binding energies of  
Zn 2p<sub>3/2</sub> and Zn 2p<sub>1/2</sub>, respectively, indicating the existence of  
Zn(II) and discarding the possible presence of oxidized  
minority species.<sup>40,41</sup> The value of ca. 161.2 eV is in good  
agreement with the S 2p<sub>3/2</sub> typical value for ZnS.<sup>40</sup> In contrast,  
a significant difference can be observed for C 1s XPS region.  
All samples show the dominant typical C-C contribution at  
284.6 eV (C2) corresponding to adventitious C. However,  
certain differences were detected for the other C-related  
species as can be seen in the left panel of Figure 5 and Table 1.  
Carbon species evolve over the time of synthesis. The  
contribution located around 287 eV (C1), typically attributed  
to C-O, shifts to less binding energy when higher reaction  
times were used. The evolution of carbon species is even more  
evident for the contribution situated at less energy with respect  
to the C-C bond (C3). These unexpected contributions were  
detected at 281.2 and 279.9 for ZnS-1h and ZnS-3h,  
respectively, and could be associated with an interaction  
between C and Zn species. The detected modifications of  
carbon-related species on the surface of ZnS have also a certain  
influence on the final carbon content of the samples. C/Zn  
ratio indicated that cleaner carbon samples can be obtained  
using longer reaction times. This fact had a relative influence  
on the final catalytic properties through the series as discussed  
in further sections.

Physisorption experiments were carried out in order to  
determine the specific surface area of the materials by nitrogen  
adsorption–desorption measurements. The samples were  
observed to be low porous materials with surface areas of 50  
m<sup>2</sup>/g, 53 m<sup>2</sup>/g, and 57 m<sup>2</sup>/g for ZnS-1h, ZnS-3h, and ZnS-5h,  
respectively. The so-obtained values showed a linear and small  
increment of the surface area increasing the reaction time. This  
relation can be correlated to the lower content of carbon  
observed in XPS analysis (Table 1). In addition, the values  
obtained for samples ZnS-1h and ZnS-3h were similar, in good  
agreement with the stabilization of carbon species described in  
XPS analysis. The maximum value obtained for ZnS-5h  
confirmed the production of a material with more active  
sites on the surface.

**Catalytic Activity.** The catalytic activity of the materials  
has been investigated in two different reactions: the selective  
liquid-phase oxidation of benzyl alcohol and toluene to  
benzaldehyde. ZnS has been recently demonstrated to exhibit  
peroxidase-like activities for the degradation of H<sub>2</sub>O<sub>2</sub> into  
hydroxyl radicals (·OH), which act as oxidants for toluene and  
benzyl alcohol.<sup>42</sup> The reported mechanism for the oxidation of  
toluene 1 and benzyl alcohol 2 to benzaldehyde 3 is illustrated  
in Scheme 1.<sup>43</sup> The only detectable side product of the  
reaction was benzoic acid 4. No other products were detected.

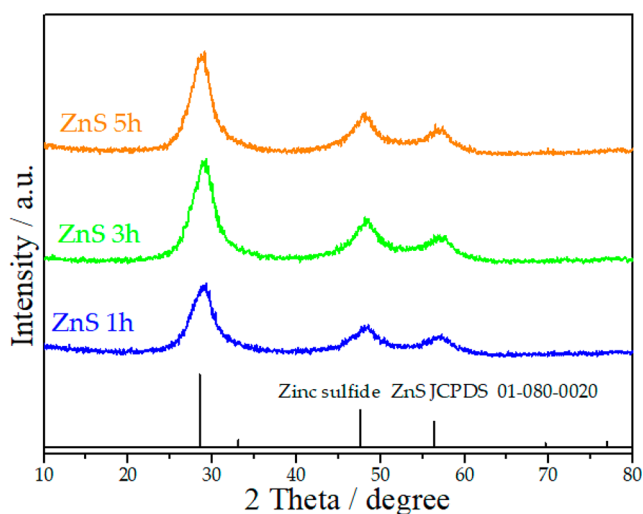


Figure 4. XRD patterns for ZnS carbon composites.



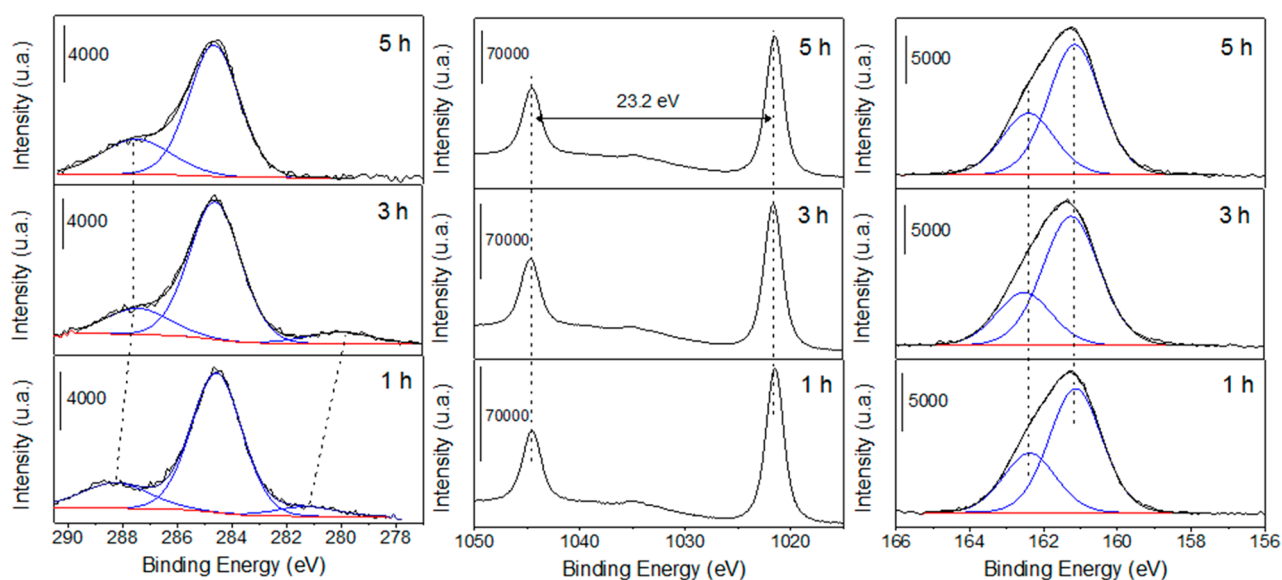


Figure 5. XPS patterns for ZnS carbon composites.

Table 1. XPS Data for ZnS Samples

sample	Zn 2p <sub>3/2</sub> (eV)	S 2p <sub>3/2</sub> (eV)	position			C/ Zn
			C 1s (eV)			
			C1	C2	C3	
ZnS-1h	1021.5	161.1	288.3	284.6	281.2	3.6
Zns-3h	1021.6	161.2	287.4	284.6	279.9	3.5
ZnS-5h	1021.5	161.2	287.5	284.6		2.2

300 The results were confirmed by a carbon balance (>95% in all  
301 tests).

302 The oxidation reaction of benzyl alcohol was carried out  
303 using the three ZnS carbon composites as heterogeneous  
304 catalysts. Results reported in Table 2 show that conversions  
305 observed were ca. ~60–65% for all ZnS carbon materials after  
306 15 min of microwave irradiation. Within the same time, the  
307 selectivity was observed to be 70%, 85%, and 87% for samples  
308 ZnS-1h, ZnS-3h, and ZnS-5h, respectively. In terms of  
309 conversion, an increase of the reaction time to 30 and 45  
310 min did not have any influence in reaction yields. Most  
311 importantly, the selectivity dropped to 64% for ZnS-1h, 82%  
312 for ZnS-3h, and 84% for ZnS-5h. On the basis of these data, all  
313 catalysts exhibited an almost identical conversion while the  
314 best selectivity was observed after 15 min employing ZnS-5h  
315 catalyst, most probably due to the larger surface area (57 g/m<sup>2</sup>  
316 vs 50 g/m<sup>2</sup> of ZnS-1h). Hypothetically, the higher surface area  
317 facilitated the rapid decomposition of H<sub>2</sub>O<sub>2</sub> into hydroxyl  
318 radicals, which directly oxidized benzyl alcohol. A lower surface  
319 area (ZnS-1h) would have taken more time to decompose  
320 hydrogen peroxide; therefore, more benzyl alcohol could have

321 been already oxidized to benzaldehyde and sequentially to  
322 benzoic acid, reducing the selectivity. In addition, sample ZnS-  
323 5h exhibited a lower C/Zn surface ratio, indicating that more  
324 active zinc sulfide sites were accessible for the degradation of  
325 hydrogen peroxide using this catalyst.

326 The stability of the catalysts was studied using the most  
327 active material ZnS-5h. The catalyst was reused up to 4 times,  
328 and the activity and selectivity to benzyl aldehyde was found to  
329 be almost identical to that of the fresh catalyst as shown in  
330 Figure 6 (for the numeric data, please see Table S1).

331 The results of the oxidation of toluene to benzaldehyde are  
332 reported in Table 3. After 15 min of reaction, the best result  
333 was obtained with ZnS-5h (19%), while the selectivity was  
334 approximately the same value (around 90%) for all three zinc  
335 sulfide carbon materials. After 30 min, an increase of  
336 conversion up to 29% with ZnS-5h was observed, while the  
337 conversion with ZnS-1h and ZnS-3h remained unchanged. On  
338 the other hand, the selectivity did not improve for any catalyst.  
339 After 45 min, the values of conversion and selectivity were  
340 equal to those obtained after 30 min, confirming that the  
341 reaction was not proceeding.

342 On the basis of these considerations, the most active catalyst  
343 was ZnS-5h, which again showed the best results after 30 min  
344 reaction. Such optimum behavior could be again explained in  
345 terms of the higher surface area and higher Zn/C ratio for  
346 ZnS-5h.

347 The stability tests were carried out using ZnS-5h. The  
348 catalyst was reused up to 4 times without any appreciable  
349 losses of activity or selectivity to benzaldehyde, as shown in  
350 Figure 7.

### Scheme 1. Proposed Mechanism for Toluene and Benzyl Alcohol Oxidation

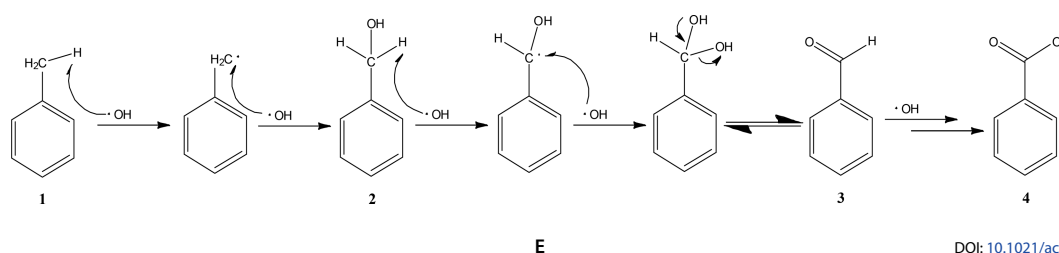


Table 2. Conversion and Selectivity Results for the Oxidation of Benzyl Alcohol

sample	15 min		30 min		45 min	
	conversion/%	selectivity/%	conversion/%	selectivity/%	conversion/%	selectivity/%
BLANK	<15	55.4	<15	53.8	<15	52.1
ZnS-1h	63.0	70.2	63.8	65.0	64.0	64.1
ZnS-3h	62.6	85.1	62.7	83.2	63.0	82.1
ZnS-5h	62.7	87.1	63.1	85.8	63.4	84.3

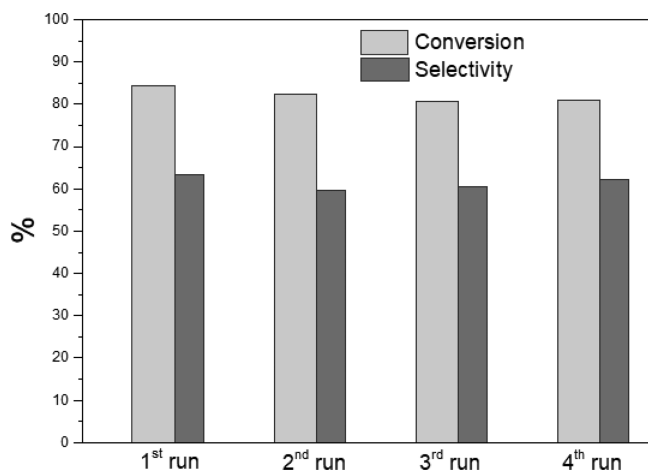


Figure 6. Schematic representation of conversion and selectivity of the most active catalyst up to the 4th run of the oxidation of benzyl alcohol.

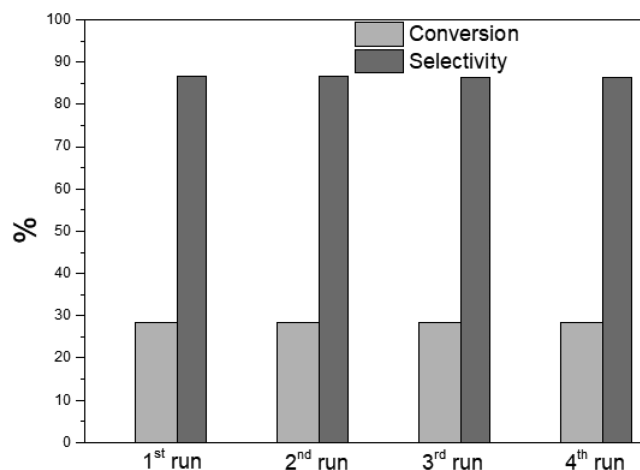


Figure 7. Schematic representation of conversion and selectivity to benzyl aldehyde for the most active catalyst up to 4th run for the oxidation of toluene (for the numeric data, please see Table S2).

## 351 ■ CONCLUSIONS

352 A simple, effective, and sustainable methodology has been  
 353 reported for the preparation of ZnS carbon composites. The  
 354 materials were synthesized using wasted pig bristles as sulfur  
 355 and carbon source and zinc acetate dihydrate as zinc precursor.  
 356 The materials were synthesized using a one step protocol  
 357 where pig bristles and zinc acetate dihydrate were heated up in  
 358 an aqueous diluted solution of KOH. The presence of zinc  
 359 sulfide phases was demonstrated by XRD and XPS analysis,  
 360 while the surface area was investigated via SEM, EDX, and N<sub>2</sub>  
 361 physisorption. The synthesis is a clear example of an easy and  
 362 sustainable valorization of wasted pig bristles. The protocol can  
 363 track new paths for substituting sulfur toxic sources with  
 364 harmless pig bristles.

365 In addition, the so-produced ZnS carbon materials showed  
 366 remarkable activity as catalysts for two different oxidation  
 367 reactions: the oxidation of benzyl alcohol to benzaldehyde and  
 368 the oxidation of toluene to benzaldehyde. The oxidation of  
 369 benzyl alcohol plays an important role in the chemical industry,  
 370 while the oxidation of toluene is extremely captivating as it  
 371 solves the problem of removing a pollutant through the  
 372 production of value-added benzyl aldehyde. For both reactions,  
 373 the most active sample was ZnS-5h, reaching the oxidation of

benzyl alcohol up to 63% with 86% selectivity and the  
 oxidation of toluene up to 29% with 87% selectivity.

## ■ ASSOCIATED CONTENT

### Supporting Information

The Supporting Information is available free of charge on the  
 ACS Publications website at DOI: 10.1021/acssuschemeng.8b04968.

Additional materials characterizations and data of the  
 reuse of the catalysts (PDF)

## ■ AUTHOR INFORMATION

### Corresponding Author

\*E-mail: q62alsor@uco.es.

### ORCID

Mario J. Muñoz-Batista: 0000-0002-1419-0592

Rafael Luque: 0000-0003-4190-1916

### Notes

The authors declare no competing financial interest.

Table 3. Conversion and Selectivity Results for the Oxidation of Toluene

sample	15 min		30 min		45 min	
	conversion/%	selectivity/%	conversion/%	selectivity/%	conversion/%	selectivity/%
BLANK	<5	~50	<5	~50	<5	~50
ZnS-1h	7.3	94.1	8.2	89.0	9.2	88.8
ZnS-3h	11.3	88.1	12.1	90.7	12.6	88.1
ZnS-5h	18.8	89.6	28.6	89.8	28.5	86.7



## 391 ■ ACKNOWLEDGMENTS

392 This project has received funding from the European Union's  
393 Horizon 2020 research and innovation programme under the  
394 Marie Skłodowska-Curie grant agreement No. 721290. This  
395 publication reflects only the author's view, exempting the  
396 Community from any liability. Project website: [http://cosmic-  
397 etn.eu/](http://cosmic-<br/>397 etn.eu/). M.J.M.-B. also thanks MINECO for the award of  
398 postdoctoral JdC contract (FJCI-2016-29014). The publica-  
399 tion has been prepared with support of RUDN University  
400 program 5-100.

## 401 ■ REFERENCES

402 (1) Fox, M. A.; Dulay, M. T. Heterogeneous photocatalysis. *Chem.*  
403 *Rev.* **1993**, *93* (1), 341–357.  
404 (2) Fang, X. S.; Bando, Y.; Gautam, U. K.; Ye, C.; Golberg, D.  
405 Inorganic semiconductor nanostructures and their field-emission  
406 applications. *J. Mater. Chem.* **2008**, *18* (5), 509–522.  
407 (3) Ummartyotin, S.; Infahsaeng, Y. A comprehensive review on  
408 ZnS: From synthesis to an approach on solar cell. *Renewable*  
409 *Sustainable Energy Rev.* **2016**, *55*, 17–24.  
410 (4) Fang, X. S.; Zhai, T. Y.; Gautam, U. K.; Li, L.; Wu, L. M.; Bando,  
411 Y.; Golberg, D. ZnS nanostructures: From synthesis to applications.  
412 *Prog. Mater. Sci.* **2011**, *56* (2), 175–287.  
413 (5) Chen, D. G.; Huang, F.; Ren, G. Q.; Li, D. S.; Zheng, M.; Wang,  
414 Y. J.; Lin, Z. ZnS nano-architectures: photocatalysis, deactivation and  
415 regeneration. *Nanoscale* **2010**, *2* (10), 2062–2064.  
416 (6) Ashkarran, A. A. Absence of photocatalytic activity in the  
417 presence of the photoluminescence property of Mn-ZnS nanoparticles  
418 prepared by a facile wet chemical method at room temperature. *Mater.*  
419 *Sci. Semicond. Process.* **2014**, *17*, 1–6.  
420 (7) Zhang, H. L.; Wei, B.; Zhu, L.; Yu, J. H.; Sun, W. J.; Xu, L. L.  
421 Cation exchange synthesis of ZnS-Ag<sub>2</sub>S microspheric composites with  
422 enhanced photocatalytic activity. *Appl. Surf. Sci.* **2013**, *270*, 133–138.  
423 (8) Vostrikov, A. A.; Fedyayeva, O. N.; Sokol, M. Y.; Shatrova, A. V.  
424 Synthesis of zinc sulfide nanoparticles during zinc oxidation by H<sub>2</sub>S  
425 and H<sub>2</sub>S/H<sub>2</sub>O supercritical fluids. *Tech. Phys. Lett.* **2014**, *40* (12),  
426 1057–1060.  
427 (9) Liu, J.; Ma, J. F.; Liu, Y.; Song, Z. W.; Sun, Y.; Fang, J. R.; Liu, Z.  
428 S. Synthesis of ZnS nanoparticles via hydrothermal process assisted by  
429 microemulsion technique. *J. Alloys Compd.* **2009**, *486* (1–2), L40–  
430 L43.  
431 (10) Biswas, S.; Kar, S.; Chaudhuri, S. Synthesis and characterization  
432 of zinc sulfide nanostructures. *Synth. React. Inorg., Met.-Org., Nano-*  
433 *Met. Chem.* **2006**, *36* (1), 33–36.  
434 (11) Zuliani, A.; Munoz-Batista, M. J.; Luque, R. Microwave-assisted  
435 valorization of pig bristles: towards visible light photocatalytic  
436 chalcocite composites. *Green Chem.* **2018**, *20*, 3001.  
437 (12) Gachango, F. G.; Ekmann, K. S.; Frorup, J.; Pedersen, S. M.  
438 Use of pig by-products (bristles and hooves) as alternative protein raw  
439 material in fish feed: A feasibility study. *Aquaculture* **2017**, *479*, 265–  
440 272.  
441 (13) Laba, W.; Kopec, W.; Chorazyk, D.; Kancelista, A.; Piegza, M.;  
442 Malik, K. Biodegradation of pretreated pig bristles by *Bacillus cereus*  
443 B5esz. *Int. Biodeterior. Biodegrad.* **2015**, *100*, 116–123.  
444 (14) Matsumoto, T.; Ueno, M.; Wang, N.; Kobayashi, S. Recent  
445 advances in immobilized metal catalysts for environmentally benign  
446 oxidation of alcohols. *Chem. - Asian J.* **2008**, *3* (2), 196–214.  
447 (15) Pineda, A.; Balu, A. M.; Campelo, J. M.; Romero, A. A.;  
448 Carmona, D.; Balas, F.; Santamaria, J.; Luque, R. A Dry Milling  
449 Approach for the Synthesis of Highly Active Nanoparticles Supported  
450 on Porous Materials. *ChemSusChem* **2011**, *4* (11), 1561–1565.  
451 (16) Gritter, R. J.; Dupre, G. D.; Wallace, T. J. Oxidation of benzyl  
452 alcohols with manganese dioxide. *Nature* **1964**, *202* (492), 179–181.  
453 (17) Yang, Z. J.; Ji, H. B. Synergistic effect of hydrogen bonding  
454 mediated selective synthesis of benzaldehyde in water. *Chin. J. Catal.*  
455 **2014**, *35* (4), 590–598.

(18) Zhu, L.; Xu, X. H.; Zheng, F. P. Synthesis of benzaldehyde by  
Swern oxidation of benzyl alcohol in a continuous flow microreactor  
system. *Turk. J. Chem.* **2018**, *42* (1), 75–85.  
(19) Colmenares, J. C.; Ouyang, W.; Ojeda, M.; Kuna, E.;  
Chernyayeva, O.; Lisovytskiy, D.; De, S.; Luque, R.; Balu, A. M.  
Mild ultrasound-assisted synthesis of TiO<sub>2</sub> supported on magnetic  
nanocomposites for selective photo-oxidation of benzyl alcohol. *Appl.*  
*Catal., B* **2016**, *183*, 107–112.  
(20) Magdziarz, A.; Colmenares, J. C.; Chernyayeva, O.;  
Kurzydowski, K.; Grzonka, J. Iron-Containing Titania Photocatalyst  
Prepared by the Sonophotodeposition Method for the Oxidation of  
Benzyl Alcohol. *ChemCatChem* **2016**, *8*, 536–539.  
(21) Magdziarz, A.; Colmenares, J. C.; Chernyayeva, O.; Lisovytskiy,  
D.; Grzonka, J.; Kurzydowski, K.; Freindl, K.; Korecki, J. Insight into  
the synthesis procedure of Fe<sup>3+</sup>/TiO<sub>2</sub>-based photocatalyst applied in  
the selective photo-oxidation of benzyl alcohol under sun-imitating  
lamp. *Ultrason. Sonochem.* **2017**, *38*, 189–196.  
(22) Ouyang, W.; Reina, J. M.; Kuna, E.; Yepez, A.; Balu, A. M.;  
Romero, A. A.; Colmenares, J. C.; Luque, R. Wheat bran valorisation:  
Towards photocatalytic nanomaterials for benzyl alcohol photo-  
oxidation. *J. Environ. Manage.* **2017**, *203*, 768–773.  
(23) Borgaonkar, H. V.; Raverkar, S. R.; Chandalia, S. B. Liquid-  
phase oxidation of toluene to benzaldehyde by air. *Ind. Eng. Chem.*  
*Prod. Res. Dev.* **1984**, *23* (3), 455–458.  
(24) Wang, Y.; Li, H. R.; Yao, J.; Wang, X. C.; Antonietti, M.  
Synthesis of boron doped polymeric carbon nitride solids and their  
use as metal-free catalysts for aliphatic C-H bond oxidation. *Chem. Sci.*  
**2011**, *2* (3), 446–450.  
(25) Andrews, L. S.; Lee, E. W.; Witmer, C. M.; Kocsis, J. J.; Snyder,  
R. Effects of toluene on metabolism, disposition and hematopoietic  
toxicity of benzene-H-3. *Biochem. Pharmacol.* **1977**, *26* (4), 293–300.  
(26) Yuan, Z. H.; Chen, B. Z.; Zhao, J. S. Controllability analysis for  
the liquid-phase catalytic oxidation of toluene to benzoic acid. *Chem.*  
*Eng. Sci.* **2011**, *66* (21), 5137–5147.  
(27) He, A.; Zhang, J.; Zheng, W. J.; Huang, C.; Zhang, C. H.;  
Huang, L. H.; Lou, J. D. Rapid oxidation of alcohols to aldehydes and  
ketones with chromium trioxide catalyzed by kieselguhr under  
solvent-free conditions. *Res. Chem. Intermed.* **2013**, *39* (3), 1015–  
1020.  
(28) Shaabani, A.; Mirzaei, P.; Lee, D. G. The beneficial effect of  
manganese dioxide on the oxidation of organic compounds by  
potassium permanganate. *Catal. Lett.* **2004**, *97* (3–4), 119–123.  
(29) Chang, C. K.; Sheldon, R. A.; Kochi, J. K. Metal-catalyzed  
oxidations of organic-compounds. *J. Am. Chem. Soc.* **1983**, *105* (11),  
3749–3749.  
(30) Gonzalo, M.; Jespersen, C. M.; Jensen, K.; Støier, S.; Meinert,  
L. Pig Bristles – An Underestimated Biomass Resource. In *62nd*  
*International Congress of Meat Science and Technology*, Bangkok,  
Thailand, Aug 14–19, 2016; Elsevier, 2016.  
(31) Mangin, F.; Prinsen, P.; Yepez, A.; Gilani, M.; Xu, G. B.; Len,  
C.; Luque, R. Microwave assisted benzyl alcohol oxidation using iron  
particles on furfuryl alcohol derived supports. *Catal. Commun.* **2018**,  
*104*, 67–70.  
(32) Dey, S. K.; Mukherjee, A. Catechol oxidase and phenoxazinone  
synthase: Biomimetic functional models and mechanistic studies.  
*Coord. Chem. Rev.* **2016**, *310*, 80–115.  
(33) Clay, R. C.; Cook, K.; Routh, J. I. Studies in the Composition  
of Human Hair. *J. Am. Chem. Soc.* **1940**, *62*, 2709.  
(34) Rechiche, O.; Plowman, J. E.; Harland, D. P.; Lee, T. V.; Lott, J.  
S. Expression and purification of high sulfur and high glycine-tyrosine  
keratin-associated proteins (KAPs) for biochemical and biophysical  
characterization. *Protein Expression Purif.* **2018**, *146*, 34–44.  
(35) Brebu, M.; Spiridon, I. Thermal degradation of keratin waste. *J.*  
*Anal. Appl. Pyrolysis* **2011**, *91* (2), 288–295.  
(36) Yeh, C. Y.; Lu, Z. W.; Froyen, S.; Zunger, A. Zinc-blende-  
wurtzite polytypism in semiconductors. *Phys. Rev. B: Condens. Matter*  
*Mater. Phys.* **1992**, *46* (16), 10086–10097.  
(37) Otto, T. N.; et al. Catalyst Characterization with FESEM/EDX  
by the Example of Silver-Catalyzed Epoxidation of 1,3-Butadiene. In

- 525 *Scanning Electron Microscopy*; Kazmiruk, V., Ed.; IntechOpen:  
526 London, 2012.
- 527 (38) *Criteria for a Recommended Standard: Occupational Exposure to*  
528 *Sodium Hydroxide*; DHHS Publication Number 76-105; NIOSH,  
529 1975.
- 530 (39) Xu, X.; Hu, L.; Gao, N.; Liu, S.; Wageh, S.; Al-Ghamdi, A. A.;  
531 Alshahrie, A.; Fang, X. Controlled Growth from ZnS Nanoparticles to  
532 ZnS–CdS Nanoparticle Hybrids with Enhanced Photoactivity. *Adv.*  
533 *Funct. Mater.* **2015**, *25* (3), 445–454.
- 534 (40) Yu, J. G.; Zhang, J.; Liu, S. W. Ion-Exchange Synthesis and  
535 Enhanced Visible-Light Photoactivity of CuS/ZnS Nanocomposite  
536 Hollow Spheres. *J. Phys. Chem. C* **2010**, *114* (32), 13642–13649.
- 537 (41) Wanger, C. D.; Riggs, W. M.; Davis, L. E.; Moulder, J. F.;  
538 Muilenberg, G. E. *Handbook of X-ray photoelectron spectroscopy: A*  
539 *reference book of standard data for use in X-ray photoelectron*  
540 *spectroscopy*; Perkin-Elmer Corp.: Eden Prairie, MN, 1979.
- 541 (42) Ding, Y. Y.; Sun, L. F.; Jiang, Y. L.; Liu, S. X.; Chen, M. X.;  
542 Chen, M. M.; Ding, Y. N.; Liu, Q. Y. A facile strategy for the  
543 preparation of ZnS nanoparticles deposited on montmorillonite and  
544 their higher catalytic activity for rapidly colorimetric detection of  
545 H<sub>2</sub>O<sub>2</sub>. *Mater. Sci. Eng., C* **2016**, *67*, 188–194.
- 546 (43) Ramu, R.; Wanna, W. H.; Janmanchi, D.; Tsai, Y. F.; Liu, C. C.;  
547 Mou, C. Y.; Yu, S. S. F. Mechanistic study for the selective oxidation  
548 of benzene and toluene catalyzed by Fe(CLO<sub>4</sub>)<sub>2</sub> in an H<sub>2</sub>O<sub>2</sub>-H<sub>2</sub>O-  
549 CH<sub>3</sub>CN system. *Mol. Catal.* **2017**, *441*, 114–121.